Journal of the Korean Physical Society, Vol. 44, No. 4, April 2004, pp. 854∼858

# Optimal Thickness Variation of an Inflatable Circular Membrane Mirror

Mingwan Soh*
*Hyun-Dae Motors, Ulsan 683-791*

Jun Ho Lee†
*Satellite Technology Research Center, Korea Advanced Institute of Science and Technology, Daejeon 305-701*

Sung-Kie Youn‡
*Department of Mechanical Engineering, Korea Advanced Institute of Science and Technology, Daejeon 305-701*

(Received 13 January 2004)

This study focuses on the optimal thickness variation of a large inflatable parabolic mirror. The inflatable mirror consists of two circular membranes joined at their edges. One membrane serves as an optical window while the other serves as an optical reflector. The membranes are shaped by pressurizing the inner space bounded by the two membranes. In this study, the thickness of the optical membrane is optimized by minimizing the root-mean-square (RMS) surface profile deviation from an ideal parabola. This study optimizes the membrane mirror by using a finite-element analysis of the membranes, in contrast to the previous membrane optimization, which utilized the mathematical theory of membrane mirrors. This study finds that a simple thickness variation does not improve the surface shapes up to the conventional requirements for visible wavelengths (RMS l/20). However, the study demonstrates that the RMS surface error of the inflatable mirror can be reduced to 1 wave in visible passbands by limiting the effective optical surface area, thus demonstrating that this mirror can be used as a primary mirror in infrared bands.

PACS numbers: 42
Keywords: Inflatable mirror, Large optics

## I. INTRODUCTION

Due to atmospheric turbulence, large optics located on the ground can achieve diffraction-limited resolving power only with adaptive optics [1]. In spite of promising developments in the field of adaptive optics, the absence of atmospheric turbulence in space is still attractive to many astronomical fields, which motivated development of the Hubble Space Telescope [2] and the Next Generation Space Telescope [3]. However, the aperture size of space optics is severely limited (up to 4 meters) by the faring size of currently available launch vehicles. In order to overcome this size limitation, two approaches have been studied: deployable [2] and inflatable optics [4–10]. As the aperture diameter of optics becomes larger (10-100 meters), inflatable optics, which have yet to be implemented in visible passands, become more attractive than deployable optics in terms of simplicity of mechanism, mass, and initial size. It is also notable that an identical concept has been used in inflating RF antennas [11].

Figure 1 shows the schematics of an inflatable mirror. Two circular membranes are joined on their boundaries and the space between them is subsequently pressurized: each membrane is inflated by pressure applied between the two membranes. One membrane serves as a window membrane through which light can transmit, and the other serves as a mirror membrane, which concentrates the light.

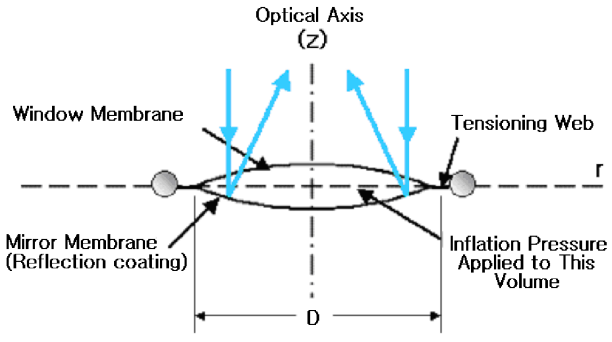


Fig. 1. Schematics of the inflatable mirror [10].

*E-mail: mgsoh@hyundai-motor.com
†E-mail: jhl@satrec.kaist.ac.kr
‡E-mail: skyoun@sorak.kaist.ac.kr

An inflatable membrane mirror was believed to be unsuitable for imaging in the visible bands until Meinel and Meinel [10] showed that varying membrane thickness could correct the classical Henky [12] aspheric shape (the so-called 'Hencky curve') of membrane mirrors for use in visible passbands. Meinel and Meinel equated the theory of variable membrane thickness and said that a unique quadratic radial variation of thickness corrects the 4-th order Hencky term. The classical Hencky curve and ideal paraboloid.are presented in Eqs. (1) and (2), and thickness variation of Meninel and Meinel is shown in Eq. (3):

$$Z_{Hencky}(u) = C(u^2 + 0.1111u^4), \tag{1}$$

$$Z_{Paraboloa}(u) = C(u^2 + 0.0000u^4), \tag{2}$$

$$t(u) = t_o(1 + 0.44u^4), \tag{3}$$

where $z$ is the sag of the membrane surface, $u$ the fractional distance from the center of the membrane, C a constant which is a function of material properties and pressure, $t$ the thickness variation in the radial direction, and $t_o$ the membrane thickness at the center.

In our research, in order to expand upon the work of Meinel and Meinel, we first optimized the thickness variation in the radial direction, performing a finite-element (FE) analysis of the membrane mirror. In addition, we investigated limiting the effective area of the membrane as a means to secure the effective area as an ideal parabola in visible passbands.

## II. OPTIMIZATION OF THE RADIAL VARIATION OF THICKNESS

### 1. Membrane Mirror Model and Optimization Procedure

The membrane models in this study are adopted from the prototype used for the inflatable antenna experiment [11]. The membranes are 3 m in diameter and are made of Kapton: Young's modulus (E) = 5.516 GPa, Poisson's ratio (n) = 0.3 and coefficient of thermal expansion = $1.210^{-5}$/C. For simplicity of the calculation, the rotationally-symmetric membrane is simulated by a 1/360 model of 200 quadrilateral 4-node elements (Fig. 2).

The optimization procedure is iterated as in Fig. 3. First, the initial values of thickness variation are determined. The analysis is then executed using commercial software: I-DEAS for pre- and post-processing and ABAQUS for solving. Then the objective function ($E_{rms}$), which is the RMS surface deviations from the ideal parabolic, is generated. The sensitivity evaluated by the finite difference method renews the values of the thickness to improve the performance. Then, the objective function is regenerated with new values of the thickness. In this process, the optimization procedure is repeated until the convergence is satisfactory.

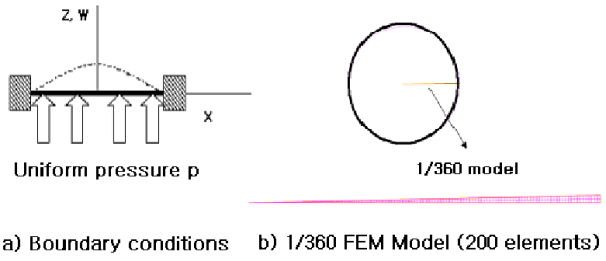


Fig. 2. Boundary conditions and model.

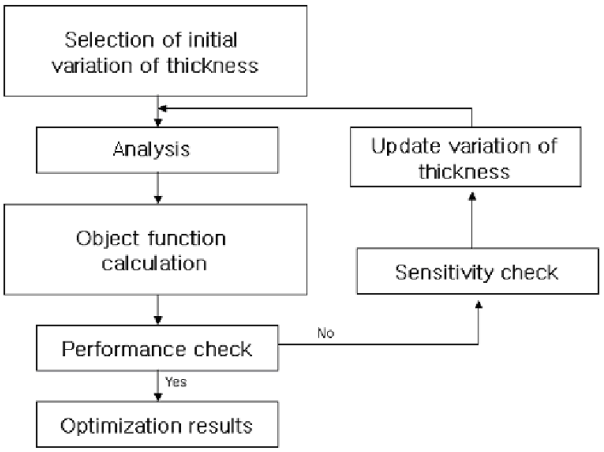


Fig. 3. Optimization procedure.

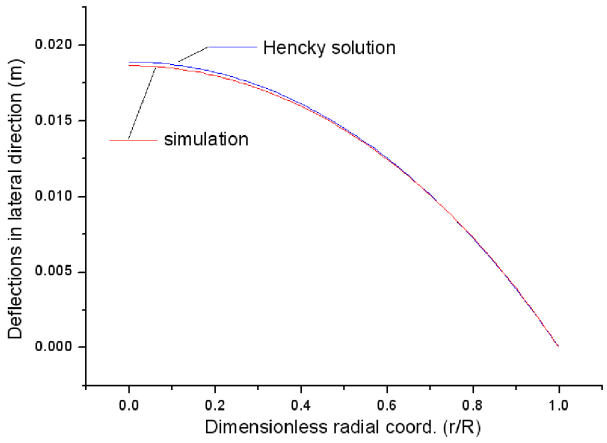


Fig. 4. Deflections in the lateral direction calculated by using Hencky's equation and by a simulation.

Before beginning the optimization, a membrane with uniform thickness was analyzed in order to confirm the validity of the model. Comparing the results and Henky's solution, we confirmed the validity of the model. Figure 4 shows the deflections of the membrane calculated by using the Henky solution and the analysis.

Table 1. Optimized thickness profiles and corresponding RMS surface (wavefront) errors.

| Thickness variation | Equation | RMS surface error |
|---|---|---|
| Uniform | $t_0 = 13.99\ \mu$m | 269 $\mu$m |
| Linear | $t = 1.89u + 13.34\ \mu$m | 261 $\mu$m |
| Parabolic | $t = 11.0(1 + 0.72u^2)\ \mu$m | 193 $\mu$m |
| Ref. 10 | $t = 12.7(1 + 0.44u^2)\ \mu$m | 302 $\mu$m |

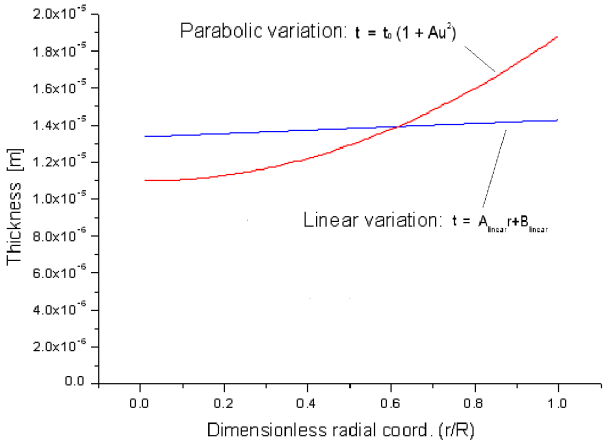


Fig. 5. Optimized membrane thickness variations: linear and parabolic.

## 2. Thickness Optimization: Uniform, Linear, and Parabolic Variation

As an initial step, membrane mirrors with three basic thickness variations are assessed: a) a uniform thickness variation (Eq. (4)), b) a linear thickness variation (Eq. (5)), and c) a parabolic thickness variation (Eq. (6)):

$$t(u) = t_0, \tag{4}$$

$$t(u) = A_{linear}u + B_{linear}, \tag{5}$$

$$t(u) = t_0(1 + A^2), \tag{6}$$

where u is the fractional distance from the center of the membrane. Table 1 summarizes the optimized thickness variations and corresponding RMS surface (wavefront) deviations from the ideal parabolic. In addition to the optimization, we performed an analysis of the membrane of Meinel and Meinel [10]. Figure 5 shows the optimized linear and parabolic thickness variations. FIG. 6 shows deviations of the membranes from the ideal parabolic. From the results, solution of Meinel and Meinel is found to be worse than the optimized membrane with a uniform thickness. In addition, the RMS surface errors of all four cases are too large (>300 waves) for a parabolic in visible passbands.

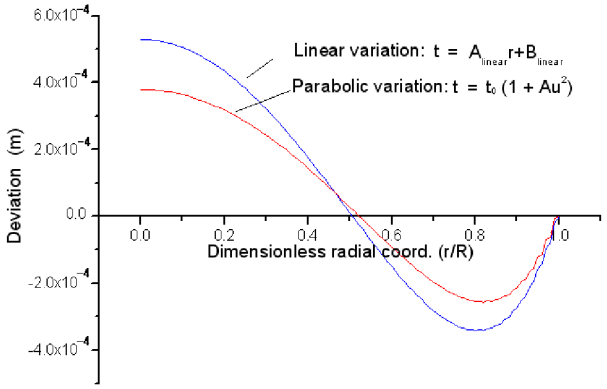


Fig. 6. Deviations from the ideal parabolic of membranes optimized by using linear and parabolic thickness variations.

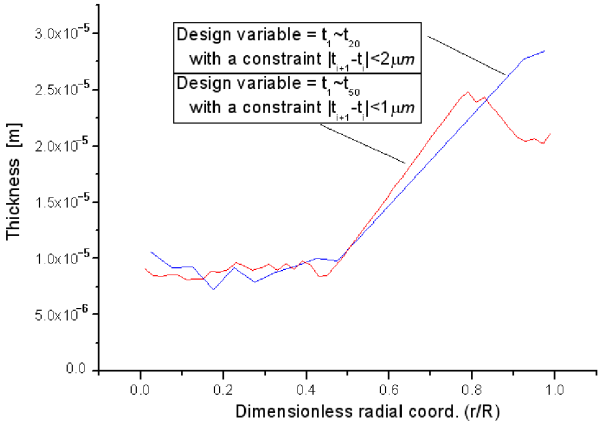


Fig. 7. Optimized membrane thickness variations using 20 and 50 discrete zonal variations.

## 3. Thickness Optimization: General Aspheric Variation

In the next step, membrane mirrors with general aspheric thickness variations are assessed: a) a discrete zonal thickness variation (Eq. (7)), and b) an even aspheric thickness variation (Eq. (8)):

$$t(u) = \begin{cases} t_1 & when \quad 0 < u < u_1 \\ \vdots & \vdots \quad\quad \vdots \\ t_n & when \quad u_{n-1} < u < u_n \\ \vdots & \vdots \quad\quad \vdots \\ t_N & when \quad u_{N-1} < u < 1, \end{cases} \tag{7}$$

$$t(u) = \sum_{i=0} A_i u^{2i}, \tag{8}$$

where u is the fractional distance from the center of the membrane, $t_i$ the thickness of the $i^{th}$ zone, N the number of zones, and $A_i$ the coefficient of even aspheric terms.

Figure 7 shows optimized thickness variations composed of discrete zonal (20 and 50) variations. When

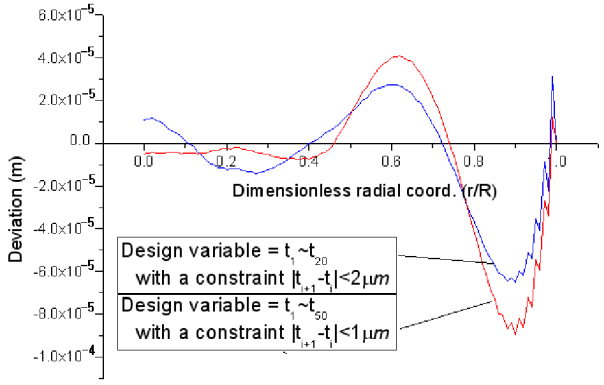


Fig. 8. Deviations from the ideal parabolic of membranes optimized by using 20 and 50 discrete zonal thickness variations.

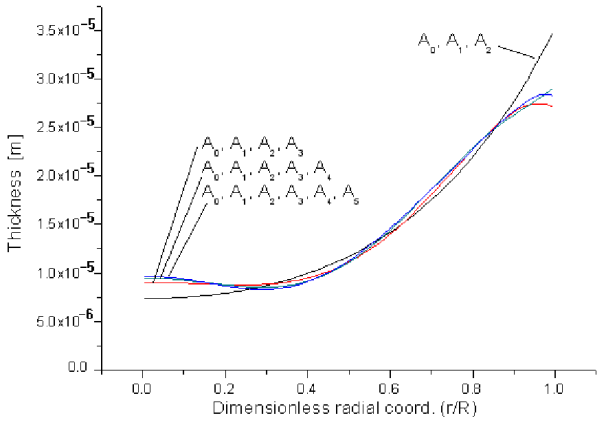


Fig. 9. Optimized membrane thickness variations obtained by using even aspheric terms.

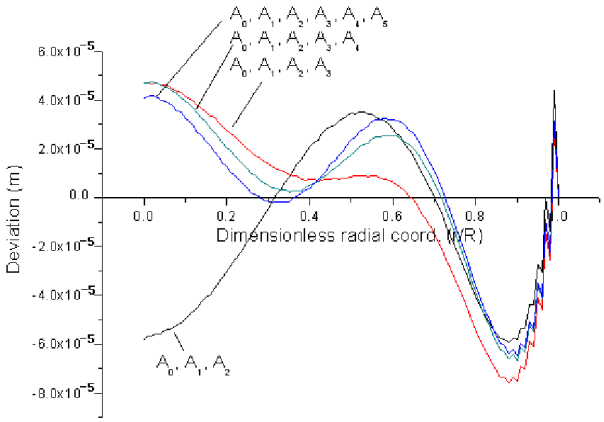


Fig. 10. Deviations from the ideal parabolic of membranes optimized by using even aspheric thickness variations.

the optimizations for two different thickness step numbers are performed, the thickness differences between two adjacent zones are constrained to be smaller than 2 $\mu$m and 1 $\mu$m, respectively. The RMS surface errors of both membranes are larger than 34 $\mu$m (50 waves).

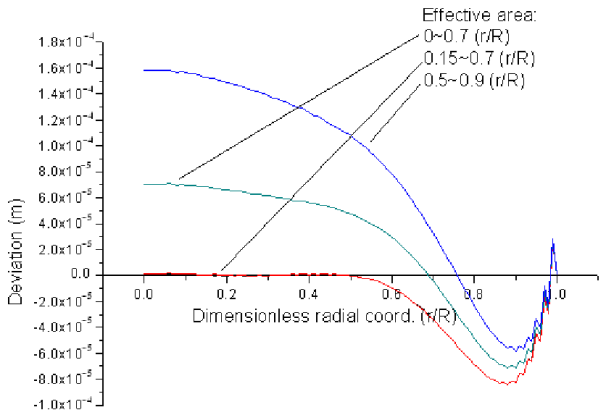


Fig. 11. Deviations from the ideal parabolic of membranes optimized by using even aspheric thickness variations when the effective apertures are limited.

For ease of implementing the thickness variation, the next optimization is performed for even aspheric thickness variations with up to 6 variables. As shown in Figs. 9 and 10, the optimized overall profiles of thickness variations are similar to those optimized from discrete zones. The RMS surface errors from this optimization are also larger than 34 $\mu$m (50 waves).

### 4. Thickness Optimization: Aperture Limitation and Even Aspheric Variation

From the previously performed optimizations, we find that the inflatable membrane mirrors have RMS surface errors larger than 50 waves in visible passbands. However, inspection of the deviation profiles of the membrane, which have dominant errors at the edges, indicates that the membrane mirror may be adequate if the effective aperture size is limited. Therefore, we performed a thickness optimization with 5 even aspheric terms while limiting the effective aperture size. Figure 11 shows the deviations profiles from the ideal parabolic of membranes optimized by even aspheric thickness variations when effective apertures are limited. Table 2 summarizes the RMS surfaces errors over full and effective apertures when the membranes are optimized over effective apertures. From this optimization, the RMS surface error can be reduced to 1 wave in visible passbands, thus opening the possibility of using the membrane mirrors in visible passbands.

## III. CONCLUSIONS

This study addresses the optimization of the thickness variation in a pressurized membrane used for a large optical system. We initially validate our model by compar-

Table 2. RMS surface (wavefront) errors when the effective areas are limited.

| Effective area (in unit of 'u') | RMS surface error over full area | RMS surface error over effective area |
|---|---|---|
| 0-0.5 | 45.6 $\mu$m | 0.74 $\mu$m |
| 0-0.6 | 46.0 $\mu$m | 2.38 $\mu$m |
| 0-0.7 | 45.2 $\mu$m | 10.1 $\mu$m |
| 0-0.8 | 44.0 $\mu$m | 26.5 $\mu$m |
| 0.15-0.6 | 46.0 $\mu$m | 3.19 $\mu$m |
| 0.15-0.7 | 45.2 $\mu$m | 12.8 $\mu$m |
| 0.15-0.8 | 43.8 $\mu$m | 32.4 $\mu$m |
| 0.5-0.9 | 48.8 $\mu$m | 33.2 $\mu$m |

ing Hencky's equation and our analysis; then, we optimize the thickness variations in five different ways: a) uniform, b) linear, c) parabolic, d) discrete zonal, and e) even aspheric. From the analysis results, the simple variation of thickness is found to be not promising in visible passbands in comparison to the conclusion in Ref. 10. However, we show that, if the effective aperture size of the membrane mirror is limited, it can be used in infrared observations. For a wavelength of around 10 $\mu m$, the RMS surface error can be reduced to RMS $\lambda/14$. Further research should follow on the matching the inflation characteristics of the membrane and the membrane plus the coating, which will be deposited on the membrane mirror surface, as well as investigation into the manufacturing procedures of the proposed membranes. Performance enhancement by using adaptive optics [13] will also be followed.

## ACKNOWLEDGMENTS

The authors are grateful to the Satellite Technology Research Center (SaTReC), Korea Advanced Institute of Science and Technology (KAIST), for sponsoring the present research work.

## REFERENCES

[1] J. M. Beckers, Annual Review of Astronomy and Astrophysics **31**, 13 (1993).
[2] M. Voit, *Hubble Space Telescope: New Views of the Universe* (Firefly Books, 2003).
[3] J. C. Mather, B. D. Seery and P. Y. Bely, Proc. SPIE **2807**, 98 (1996).
[4] R. D. Kornbluh, D. S. Flamm, H. Prahad, K. M. Nashold, S. Chhokar, R. Pelrine, D. L. Huestis, J. Simons, T. Cooper and D. G. Watters, Proc. SPIE **5051**, 143 (2003).
[5] E-H. Yang and K. Shcheglov, Proc. SPIE **4839**, 703 (2003).
[6] E. P. Maqee, M. C. Roggemann and A. S. Kondrath, Proc. SPIE **4824**, 72 (2002).
[7] K. Lee and T. C. Phong, J. Korean Phys. Soc. **43**, 807(2003).
[8] C. H. Jenkins and D. K. Marker, Transactions of the ASME **120**, 298 (1998).
[9] G. Greschik and M. M. Mikulas, AIAA **39**, 308 (2001).
[10] A. B. Meinel and M. P. Meinel, Opt. Eng. **39**, 541 (2000).
[11] R. E. Freeland and G. Bilyeu, Acta Astronautica **30**, 29 (1993).
[12] H. Henky and Z. Math. Phys. **63**, 311 (1915).
[13] S-K. Park, S-H. Baik, Y-S. Seo, C-J. Kim and S. W. Ra, J. Korean Phys. Soc. **42**, 743 (2003).